Q. J. R. Meteorol. Soc. (1993), **119**, pp. 547–565 551.509.33

An analogue–dynamical long-range numerical weather prediction system incorporating historical evolution

By HUANG JIANPING*†, YI YUHONG†, WANG SHAOWU
Department of Geophysics, Peking University, Beijing 100871, *P.R.C.*

and

CHOU JIFEN
Department of Atmospheric Science, Lanzhou University, Lanzhou 730001, *P.R.C.*

(Received 3 December 1990; revised 29 June 1992)

SUMMARY

It is convenient to regard a predicted dynamical field as a small disturbance superimposed on a historical analogue field. A statistical technique can then be used in combination with a dynamical forecast. Using this approach, a coupled atmosphere/earth-surface analogue–dynamical model has been formulated and applied to seasonal prediction. This approach facilitates the use of information contained both in the historical data-set and in the initial field in improving the dynamical model (based solely on the latter) and shows some predictive skill.

1. INTRODUCTION

Forecasts for a month or a season ahead are currently being carried out on a routine operational basis using statistical methods, but the results exhibit only marginal skill (Nicholls 1984; Nap *et al.* 1981). Consideration has thus been given to the use of comprehensive global circulation models (GCMs) for forecasts of this range, although preliminary attempts based on simple models have also been tried (e.g. Chao *et al.* 1982; Miyakoda and Chao 1982). At present, however, forecasts for one month ahead with GCMs are in the experimental stage. Knowledge concerning, and experience in the use of, GCMs for seasonal and long-range forecasting is still very meagre.

The limitations of current anomaly methods of long-range forecasting are widely acknowledged; in principle, with them it is not possible to distinguish between physical and random relationships in the data and therefore recourse has to be made to the laws of physics. On the other hand, purely dynamical methods of long-range numerical weather prediction (NWP) encounter difficulties for the following reasons (Chou 1986a).

(a) The temperature of the active layer of the ocean is important as an initial condition but it is inadequately observed.

(b) Parametrizations are beset by inevitable deficiencies.

(c) Prediction concerning the atmosphere is an indeterminate initial-value problem.

Since the purely statistical and purely dynamical methods have their own particular shortcomings, it is necessary to seek other ways, such as combining both methods together (Nicholls 1984). Several dynamical–statistical models have already been developed. However, it may be that methods involving both statistical and dynamical methods are not as efficient as a purely statistical or purely dynamical technique on its own. It is therefore necessary to investigate how best to combine the two methods.

It is natural to consider long-range forecasting as a problem in information processing (Chou 1986a,b). The task in long-range forecasting consists in estimating the future by

* Corresponding author.
† Present address: Climate System Research Program, College of Geosciences and Maritime Studies, Texas A and M University College Station, TX 77843-3150, U.S.A.

using physical laws together with all the available data, comprising historical records, current observations and all information extracted from these data. In other words, although it is not possible to formulate accurately equations governing long-range weather prediction, the observational data for the atmosphere provided by the global observing network in fact contain particular solutions of these equations. Therefore it should be possible by making use of this information to remedy the defects of the models and so to improve numerical weather prediction.

Evolution analogues can be found for states in both atmosphere and ocean. Therefore, historical analogues are still one of the most widely applied methods in present-day seasonal prediction. Researchers have demonstrated some skill using such methods (Nicholls 1984; Murray 1977; Schuurmans 1973; Nap *et al.* 1981; Wang *et al.* 1987). However, this technique supposes that the future evolution is a repetition of the past, which in practice is obviously not the case. The combination of analogue and dynamical methods, by means of viewing the field to be predicted as a small disturbance superimposed on a historical analogue, should help to include the rich experience of statistical forecasting within a numerical prediction model. The analogue–dynamical seasonal numerical prediction model that we now introduce below is based on this idea.

In section 2 we first review the analogue approach in long-range prediction, and in section 3 discuss the basic principles of the analogue–dynamical approach. In section 4 we introduce the equations for the analogue–dynamical model. The method of solving them is then discussed in section 5, and in section 6 we discuss the experiments on seasonal predictions; experimental predictions, from winter to summer and from summer to winter, were carried out. Section 7 concludes with a summary and a list of future work and possible useful modifications of the model.

2. The analogue approach in long-range prediction

The use of analogues has a long association with meteorology. In long-range prediction the technique consists in examining historical data, identifying one or more months or seasons that resemble the month or season just past and then predicting that the situation in the following month or season will resemble that observed during the period following the chosen 'analogue' (Nicholls 1984).

Considerable study of the potential use of analogues in long-range prediction for the British Isles has already been carried out. Some of these studies examined making use of very simple analogue selection techniques. Davis (1978a,b) used seasonal mean temperature and rainfall records (and sometimes the pressure distribution) to find analogues by which to predict English seasonal conditions. The weather predicted was that most commonly observed in the years for which the analogues had been selected. Jolliffe (1979) examined the forecasts prepared by Davis and found some skill, at least so far as the summer temperature forecasts were concerned.

The limitations of simple analogue selection procedures have led many to seek to widen the area of data used in the analogue selection. Considerable effort along these lines has been expended by the Meteorological Office where the surface atmospheric pressure and 500 hPa height fields that occur prior to a particular weather pattern have been studied. Some promising results were obtained (e.g. Ratcliffe 1968, 1974; Murray 1968, 1972, 1973, 1974; Ratcliffe and Collison 1969; Murray and Benwell 1970; Folland 1975; Lee and Ratcliffe 1976). A typical example of the forecast technique employed in these studies is that of Murray (1973) for spring rainfall in England and Wales. Murray (1977) examined the accuracy of seasonal forecasting techniques using independent data

from 1970 to 1976 (Murray 1972, 1973). Over this period the forecast rules showed skill (a conclusion also reached by Jolliffe 1979), although the number of forecasts verified was very small.

Schuurmans (1973) described a similar method for preparing monthly forecasts for the Netherlands from circulation analogues. Figure 1 shows the skill scores in forecasting monthly mean temperature, given by Nap *et al.* (1981); both yearly and cumulative values of the skill, S, are given. After M forecasts with N hits the skill core is defined as

$$S = N/M - C \tag{1}$$

where C is the climatological chance. S measures the success better than chance (a value of 25% means that out of 100 forecasts 25 were more accurate than could be expected on the basis of climatological chance). Figure 1 shows that the method has a score of almost 5% over climatology.

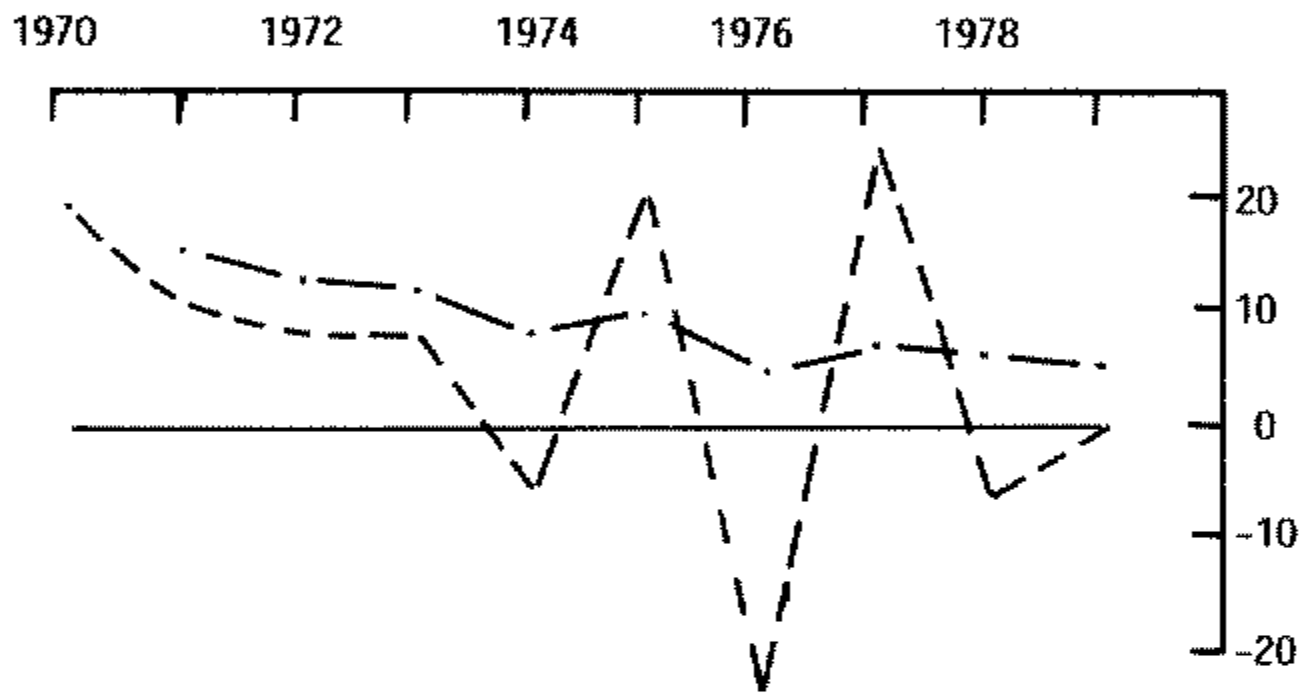

Figure 1. The verification score S (%) measuring the skill of monthly mean temperature forecasts. The dashed lines connect annual values (12 forecasts) while the dashed-dotted line represents the cumulative value of S. (From Nap *et al.* 1981).

Analogue prediction has also been studied in the former USSR with Gruza and Rankova (1980) suggesting that the use of a group of analogues (rather than the selection of a single 'best' analogue) would allow analogue probabilistic seasonal forecasts to be made.

Barnett and Preisendorfer (1978) used a variety of data including the northern hemisphere 700 hPa height, the 1000–700 hPa thickness, the air temperature, the precipitation, and the sea surface temperature in selecting analogues for the prediction of seasonal temperature in the USA. In this study a 'climate state vector', tracing the path of a 'climate particle', was used to represent the time evolution of the climate system. A variety of methods was used to select analogues, and statistically significant skill was achieved.

Long-range operational forecasting practice in China also shows that the winter circulation and surface conditions, like sea surface temperature and snow cover, are of great significance to the forecasting of summer circulation patterns and precipitation (Wang *et al.* 1987; Huang *et al.* 1990). Wang (1984) and Wang *et al.* (1987) reported their investigation of analogue evolution of the circulation anomaly (this analogue was originally used for assessing predictability by Lorenz (1969) in his investigations of medium-range weather forecasting). They found that if the January circulation anomalies in two years are analogues of each other, then the circulation anomalies will have an analogue in June or August, which can be regarded as a manifestation of rhythm in

atmospheric circulation variations. Evidently the similarity between the initial months has a seasonal prediction signal. Analogue evolution similar to that in the atmosphere is also strongly manifested in the oceans, but with a different seasonal bias.

It appears that the analogue approach can produce long-range forecasts showing a real increase in skill over a random forecast (Nicholls 1984). The major problem with this approach is the simplistic assumption that we can take the future evolution as being a repetition of a sequence of events in the past. However, it seems possible that results may be improved if we combine the analogue and dynamical approaches. Some of the fundamental principles of the analogue–dynamical model are outlined in the next section.

3. Basic principles of the analogue–dynamical approach

Long-range numerical forecasts made with standard GCMs cater not only for the prediction of anomalies but also for the simulation of seasonal variations of climate. The latter are much greater than the anomalies in the same period and even the smallest error in the seasonal climate simulation may have a great influence on the anomaly forecast. This so-called climatic drift is difficult to deal with. Therefore, models developed in recent years have separated out the mean climatic variation and the anomalies (Chao *et al.* 1977; Lin *et al.* 1988; Miyakoda and Chao 1982; Navarra and Miyakoda 1988). Since the former is known, the models are restricted to predict the latter. Numerical simulations indicate that the anomaly models are superior to standard GCMs. But in the predictive equations of an anomaly model, there will be second-order correlation terms obtained from ensemble averages (those of instantaneous eddy transfer terms), the contribution of which has not been thoroughly investigated and has been generally ignored. Yet this problem can be reduced by replacing the climatic average in the anomaly model with the evolution of the general circulation selected from the historical records, using the analogue techniques. This is referred to as the analogue–dynamical model. The analogue–dynamical model avoids simulating the mean seasonal climate variations and also the evolution provided by the analogue basic state, i.e. the analogue–dynamical model combines the advantages of the dynamical model with the analogue's selection of the evolution of the atmospheric circulation.

Generally, numerical weather prediction aims at the solution of the following Cauchy problem:

$$\frac{\partial \boldsymbol{\Psi}}{\partial t} + \mathrm{L}(\boldsymbol{\Psi}) = \mathrm{F}(\boldsymbol{\Psi}) \tag{1}$$

$$\boldsymbol{\Psi}(\mathbf{x}, 0) = \mathbf{G}(\mathbf{x}), \qquad t = 0 \tag{2}$$

where $\mathbf{x}$ is the spatial coordinate vector, $\boldsymbol{\Psi}$ is the state vector to be predicted (including the atmosphere, soil and sea temperature etc.), L is the differential operator of $\boldsymbol{\Psi}$ (usually nonlinear in character), F is the error operator of the model (like the eddy transfer term in the anomaly model equation), which is often ignored.

In the analogue–dynamical method, $\boldsymbol{\Psi}$ is divided into the basic state and the perturbation, i.e. $\boldsymbol{\Psi} = \tilde{\boldsymbol{\Psi}} + \hat{\boldsymbol{\Psi}}$, where $\tilde{\boldsymbol{\Psi}}$ is selected from historical observational records according to the similarity of $\tilde{\boldsymbol{\Psi}}(\mathbf{x}, 0)$ to the initial value $\mathbf{G}(\mathbf{x})$. The basic state is expressed by the following equations:

$$\frac{\partial \tilde{\boldsymbol{\Psi}}}{\partial t} + \mathrm{L}(\tilde{\boldsymbol{\Psi}}) = \mathrm{F}_1(\tilde{\boldsymbol{\Psi}}) \tag{3}$$

$$\tilde{\boldsymbol{\Psi}}(\mathbf{x}, 0) = \tilde{\mathbf{G}}(\mathbf{x}) \tag{4}$$

Substituting into (1) and (2), which are then subtracted from (3) and (4), respectively, we get the equations for the disturbance state, viz.

$$\frac{\partial \hat{\boldsymbol{\Psi}}}{\partial t} + \mathrm{L}(\tilde{\boldsymbol{\Psi}} + \hat{\boldsymbol{\Psi}}) - \mathrm{L}(\tilde{\boldsymbol{\Psi}}) = \mathrm{F}(\tilde{\boldsymbol{\Psi}} + \hat{\boldsymbol{\Psi}}) - \mathrm{F}_1(\tilde{\boldsymbol{\Psi}}) \tag{5}$$

$$\hat{\boldsymbol{\Psi}}(\mathbf{x}, 0) = \mathbf{G}(\mathbf{x}) - \tilde{\mathbf{G}}(\mathbf{x}) \tag{6}$$

It can be seen from the above analysis that the error term in ordinary NWP is $\mathrm{F}(\boldsymbol{\Psi})$, while it is $\mathrm{F}(\tilde{\boldsymbol{\Psi}} + \hat{\boldsymbol{\Psi}}) - \mathrm{F}_1(\tilde{\boldsymbol{\Psi}})$ for the analogue–dynamical approach. If, in selecting the basic state, we can ensure that

(a) the initial fields and boundary conditions (such as at the underlying surface) of the analogue basic state are similar to those in the forecast,

(b) the analogue basic state is in the same season as the forecast interval,

then a good approximation can be expected between $\mathrm{F}(\tilde{\boldsymbol{\Psi}} + \hat{\boldsymbol{\Psi}})$ and $\mathrm{F}_1(\tilde{\boldsymbol{\Psi}})$, i.e.

$$\|\mathrm{F}(\tilde{\boldsymbol{\Psi}} + \hat{\boldsymbol{\Psi}}) - \mathrm{F}_1(\tilde{\boldsymbol{\Psi}})\| \ll \|\mathrm{F}_1(\tilde{\boldsymbol{\Psi}})\|$$

Both F and F_1 are unknown, but the right-hand side of (5) can be assumed to be negligibly small, i.e.

$$\frac{\partial \hat{\boldsymbol{\Psi}}}{\partial t} + \mathrm{L}(\tilde{\boldsymbol{\Psi}} + \hat{\boldsymbol{\Psi}}) - \mathrm{L}(\tilde{\boldsymbol{\Psi}}) = 0 \tag{7}$$

$\hat{\boldsymbol{\Psi}}$ obtained from (6) and (7) is added to $\tilde{\boldsymbol{\Psi}}$ to produce the forecast values of $\boldsymbol{\Psi}$. This suggests that the model will have greater accuracy than either the GCM or the analogue forecasts, owing to compensating effects of errors from similar sources.

4. Description of the model

The model includes a representation of the thermodynamics of both the atmosphere and the surface. Quasi-geostrophic equations are applied for the atmosphere, and the equation of heat conduction includes oceanic advection at the sea surface. Earth–air coupling is realized through the physical processes of an energy budget at the earth–air interface. Oceanic and atmospheric states tend to follow similar evolutions with analogue initial fields and boundary conditions. Therefore, the field to be forecast is viewed as a small disturbance superimposed on historical similarity. We resolve the oceanic and atmospheric states into basic and perturbation ones. We then assume that the monthly mean variation, X, can be written

$$X = \tilde{X} + \hat{X}$$

where the basic state $\tilde{X}$ is the monthly average of a historical similarity year chosen on the basis of its analogue to the initial value, and $\hat{X}$ is called similarity deviation, or simple deviation. Putting $X = \tilde{X} + \hat{X}$ into the basic equations with the assumption that the basic state satisfies the basic equations, the equations will have their deviation form

$$\frac{\partial}{\partial t}\nabla^2\hat{\phi} + \frac{1}{f}J(\tilde{\phi}, \nabla^2\hat{\phi}) + \frac{1}{f}J(\hat{\phi}, \nabla^2\tilde{\phi}) + \frac{1}{f}J(\hat{\phi}, \nabla^2\hat{\phi}) + \frac{2\Omega}{a^2}\frac{\partial\hat{\phi}}{\partial\lambda} = f^2\frac{\partial\hat{\omega}}{\partial p} - \alpha\nabla^2\hat{\phi} \tag{8}$$

$$\frac{\partial}{\partial t}\left(\frac{\partial\hat{\phi}}{\partial p}\right) + \frac{1}{f}J\left(\tilde{\phi}, \frac{\partial\hat{\phi}}{\partial p}\right) + \frac{1}{f}J\left(\hat{\phi}, \frac{\partial\tilde{\phi}}{\partial p}\right) + \frac{1}{f}J\left(\hat{\phi}, \frac{\partial\hat{\phi}}{\partial p}\right) + \sigma_{\mathrm{p}}\hat{\omega} = -\frac{R}{p}\hat{Q} \tag{9}$$

$$\frac{\partial}{\partial t}\hat{T}_{\mathrm{s}} + \delta\left\{J_{\mathrm{s}}(\tilde{\Psi}_{\mathrm{s}}, \hat{T}_{\mathrm{s}}) + J_{\mathrm{s}}(\hat{\Psi}_{\mathrm{s}}, \tilde{T}_{\mathrm{s}}) + J_{\mathrm{s}}(\hat{\Psi}_{\mathrm{s}}, \hat{T}_{\mathrm{s}})\right\} = K_{\mathrm{s}}\frac{\partial^2\hat{T}_{\mathrm{s}}}{\partial z^2} \tag{10}$$

where

$$\nabla^2 = \frac{1}{a^2}\left(\frac{1}{\sin^2\theta}\frac{\partial}{\partial\lambda^2} + \frac{1}{\sin\theta}\frac{\partial}{\partial\theta}\sin\theta\frac{\partial}{\partial\theta}\right),$$

$$J(A, B) = \frac{1}{a^2\sin\theta}\left(\frac{\partial A}{\partial\theta}\frac{\partial B}{\partial\lambda} - \frac{\partial A}{\partial\lambda}\frac{\partial B}{\partial\theta}\right),$$

$$J_s(A., B) = \frac{2^{1/2}}{2}\frac{0.0126}{(\cos\theta)^{1/2}a^2}\left\{\left(\frac{\partial A}{\partial\theta} + \frac{1}{\sin\theta}\frac{\partial A}{\partial\lambda}\right)\frac{1}{\sin\theta}\frac{\partial B}{\partial\lambda} + \left(\frac{\partial A}{\partial\theta} - \frac{1}{\sin\theta}\frac{\partial A}{\partial\lambda}\right)\frac{\partial B}{\partial\theta}\right\}$$

(Here the term $J_s(A, B)$ is derived from oceanic advection using the Ekman wind drift formula)

$$\delta = \begin{cases} 1 & \text{for sea} \\ 0 & \text{for land} \end{cases}$$

a is the earth's radius, θ the latitude, λ the longitude, p the pressure, R the gas constant, f the Coriolis parameter, Ψ_s the surface stream function, T_s the surface temperature, K_s the heat conduction coefficient for the soil (over land) or for the upper layers of the ocean (over the sea), ρ the air density, c_p the specific heat at constant pressure, g gravity.

$$\sigma_p = \frac{R^2\tilde{T}}{gp^2}(\gamma_d - \gamma)$$

where $(\gamma_d - \gamma)$ is the difference between the dry adiabatic and the actual lapse rate. $\hat{Q} = \hat{\varepsilon}/\rho c_p$ is the deviation of diabatic heating where

$$\hat{\varepsilon} = \hat{\varepsilon}_H + \hat{\varepsilon}_R + \hat{\varepsilon}_L$$

$\hat{\varepsilon}_H$ being expressed in terms of the turbulent diffusion, viz.

$$\hat{\varepsilon}_H = \rho c_p \frac{\partial}{\partial p}\left(\rho^2 g^2 K_T \frac{\partial\hat{T}}{\partial p}\right) \tag{11}$$

where K_T is the turbulent heat conduction coefficient. The term $\hat{\varepsilon}_R$ consists of shortwave and longwave radiation components, viz.

$$\hat{\varepsilon}_R = \bar{I}(1 - c_s\hat{n})(1 - \alpha_s) + \rho c_p\left\{\frac{\partial}{\partial p}\left(p^2 g^2 K_R \frac{\partial\hat{T}}{\partial p}\right) - \frac{\hat{T}}{\tau_R}\right\} \tag{12}$$

where the shortwave radiation term involves the monthly average solar radiation, $\bar{I}$, at the top of the atmosphere, the surface albedo, α_s, and the cloudiness deviation, $\hat{n}$. The latter is parametrized as being proportional to the surface vorticity deviation, viz.

$$\hat{n} = \left(\frac{K_T}{2f}\right)^{1/2}\frac{\nabla^2\hat{\phi}_s}{f\omega_0}$$

where ω_0 is a constant. The longwave radiation is expressed, after Kuo (1969), in terms of a 'diffusive' term with coefficient K_R, and a Newtonian cooling-to-space term with time constant, τ_R. The quantity $\hat{\varepsilon}_L$ is expressed, after Smagorinsky (1969), in terms of the surface vorticity deviation, viz.

$$\hat{\varepsilon}_L = \rho L_v \gamma \frac{\partial}{\partial\bar{T}}(l_n\tilde{e}_s)\,\tilde{q}_s\left(\frac{K_T}{2f}\right)^{1/2}\frac{\nabla^2\hat{\phi}_s}{f} \tag{13}$$

where L_v is the latent heat of vaporization, e_s is the saturation vapour pressure and q_s is the specific humidity.

5. NUMERICAL SOLUTION

The atmosphere is divided into three levels (Fig. 2), and the geopotential tendency equation, obtained by eliminating $\hat{\omega}$ in (8) and (9), is given on the 300, 500 and 700 hPa levels, respectively. We assume that

$$p = 0, \qquad \hat{\omega} = 0, \qquad \left(\frac{\partial \hat{\phi}}{\partial p}\right)_0 = 0$$

$$p = p_s, \qquad \hat{\omega} = 0, \qquad \left(\frac{\partial \hat{\theta}}{\partial p}\right)_4 = -\frac{R}{p_s}\hat{T}_s$$

$$\left(\frac{\partial \hat{\phi}}{\partial p}\right)_1 = \frac{1}{\Delta p}(\hat{\phi}_2 - \hat{\phi}_1), \qquad \left(\frac{\partial \tilde{\phi}}{\partial p}\right)_1 = -\frac{R}{p_1}\tilde{T}_1,$$

$$\left(\frac{\partial \hat{\phi}}{\partial p}\right)_2 = \frac{1}{2\Delta p}(\hat{\phi}_3 - \hat{\phi}_1), \qquad \left(\frac{\partial \tilde{\phi}}{\partial p}\right)_2 = -\frac{R}{p_2}\tilde{T}_2$$

$$\left(\frac{\partial \hat{\phi}}{\partial p}\right)_3 = \frac{1}{\Delta p}(\hat{\phi}_3 - \hat{\phi}_2), \qquad \left(\frac{\partial \tilde{\phi}}{\partial p}\right)_3 = -\frac{R}{p_3}\tilde{T}_3$$

Monthly averaged geopotential anomaly fields have an equivalent barotropic structure (Blackmon *et al.* 1979; Huang *et al.* 1988), and therefore the geopotential height deviation in the 300 and 700 hPa surfaces can be expressed in terms of that of the 500 hPa surface, viz.

$$\hat{\phi}_1 = B_1\hat{\phi}_2, \qquad \hat{\phi}_3 = B_3\hat{\phi}_2,$$

where $B_i (i = 1, 3)$ are regression coefficients, so that

$$\left(\frac{\partial \hat{\phi}}{\partial p}\right)_1 = E_1\hat{\phi}_2, \qquad E_1 = \frac{1}{\Delta p}(1 - B_1)$$

$$\left(\frac{\partial \hat{\phi}}{\partial p}\right)_2 = E_2\hat{\phi}_2, \qquad E_2 = \frac{1}{2\Delta p}(B_3 - B_1)$$

$$\left(\frac{\partial \hat{\phi}}{\partial p}\right)_3 = E_3\hat{\phi}_2, \qquad E_3 = \frac{1}{\Delta p}(B_3 - 1)$$

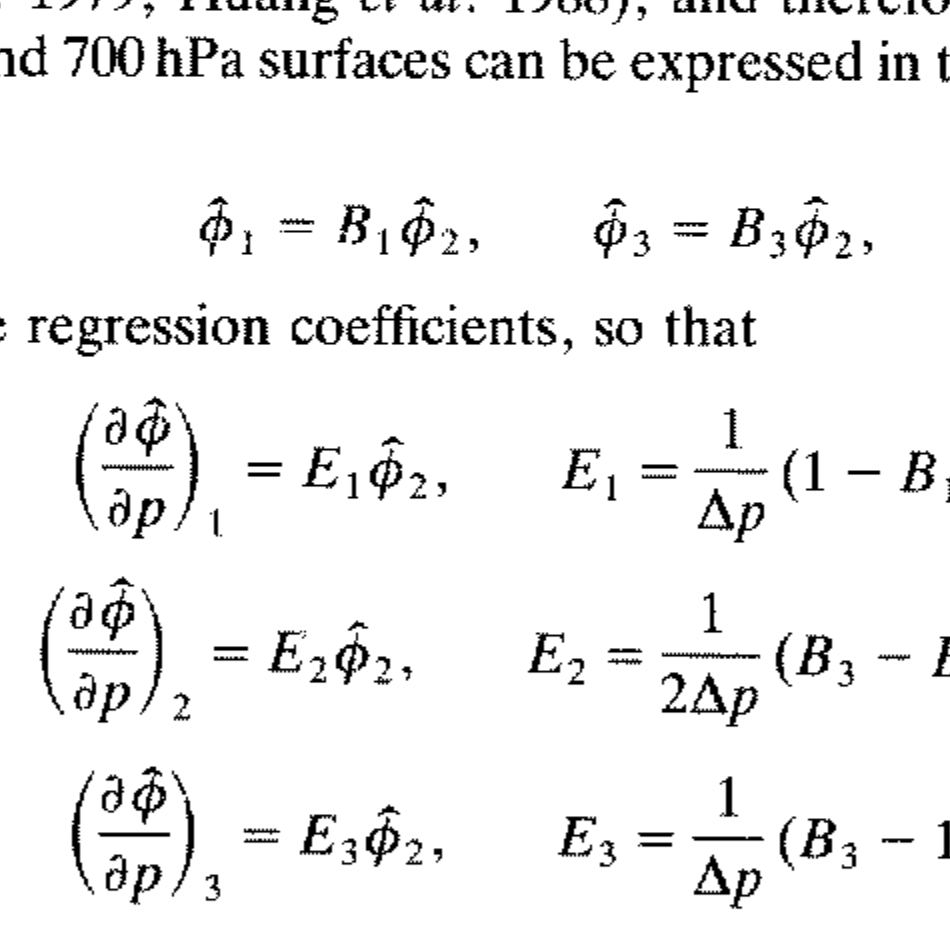

Figure 2. Schematic of the vertical structure of the model.

After manipulation, the deviation prediction equation for the model atmosphere takes the form

$$\frac{\partial}{\partial t}(\nabla^2\hat{\phi}_2 - \lambda\hat{\phi}_2) = -\mathrm{L}(\hat{\phi}_2) - \alpha\nabla^2\hat{\phi}_2 + Q_{\mathrm{A}_1}\hat{\phi}_2 + Q_{\mathrm{A}_2}\nabla^2\hat{\phi}_2 + Q_{\mathrm{s}_1}\hat{T}_{\mathrm{s}} \tag{14}$$

where

$$\mathrm{L}(\hat{\phi}_2) = \frac{1}{f}\Big\{J(\bar{\phi}_2, \nabla^2\hat{\phi}_2) + J(\hat{\phi}_2, \nabla\bar{\phi}_2) + J(\hat{\phi}_2, \nabla^2\hat{\phi}_2) + \frac{2\Omega}{a}\frac{\partial\hat{\phi}}{\partial\lambda} + J(A_1\bar{\phi}_3 - A_2\bar{\phi}_1, \hat{\phi}_2) + J(A_3\bar{T}_3 - A_4\bar{T}_4, \hat{\phi}_2)\Big\},$$

where $Q_{\mathrm{A}_1}, Q_{\mathrm{A}_2}, Q_{\mathrm{s}_1}$ are diabatic heating coefficients and

$$\lambda = \frac{f^2}{2\Delta p}\left[\frac{E_1}{\sigma_{\mathrm{p}1}} - \frac{E_3}{\sigma_{\mathrm{p}3}}\right]$$

$$A_1 = \frac{f}{2\Delta p}\cdot\frac{E_3}{\sigma_{\mathrm{p}3}}, \qquad A_2 = \frac{f}{2\Delta p}\frac{E_1}{\sigma_{\mathrm{p}3}}$$

$$A_3 = \frac{f}{2\Delta p}\frac{B_3}{\sigma_{\mathrm{p}3}}\frac{R}{p_3}, \qquad A_4 = \frac{f}{2\Delta p}\frac{B_1 R}{\sigma_{\mathrm{p}4}p_4}$$

A filtering scheme is used in the time integration of the atmospheric model, which has the form

$$Y_*^{m+1} = Y^{m-1} + 2\Delta t\frac{\partial Y^m}{\partial t} \tag{15}$$

$$Y^m = Y_*^m + \eta(Y_*^{m+1} + Y^{m-1} - 2Y_*^m) \tag{16}$$

Quantities with an asterisk are first approximation values; η is the control parameter. This scheme not only filters small-scale disturbances in the calculation, but also keeps the integration stable using a long time-step, Δt, which, for this model, is taken to be 4 hours.

Solution of the deviation equation (10) requires two boundary conditions. At the earth's surface the energy balance deviation equation is used, and at a depth D underground $\hat{T}_{\mathrm{s}}$ is taken as zero.

By means of (11) and (12), and by putting (3) into a difference equation, an approximate analytical solution to the temperature deviation at time $t + \Delta t$ in the active surface layer can be derived.

Diabatic factors are physically important in long-range forecasting. However, the related parameters in (14) i.e. $Q_{\mathrm{A}_1}, Q_{\mathrm{A}_2}, Q_{\mathrm{s}_1}$, are difficult to determine with great accuracy and the best way to solve this problem is by the so-called inversion method. Chou (1986b) proposed such a scheme for objectively determining physical parameters in numerical prediction models.

In our experiments, the parameters were determined as follows. For January 1966, the two best analogue years were chosen from the January 500 hPa and surface temperature data-set from the years 1967–1980. The differences fields between January 1966 and each analogue were then calculated. This was repeated for each January in the years 1967, 1968, . . . , 1980, the two best analogue years being chosen from the remaining fourteen years of the series. Thus 30 differences fields were obtained. These were put into (14) and produced the values of parameters $Q_{\mathrm{A}_1}, Q_{\mathrm{A}_2}, Q_{\mathrm{s}_1}$ for January. Similarly,

we also acquired the parameter values for February, March, . . . , December. These parameters varied with season and geographical distribution. It is acknowledged, however, that this technique leaves much to be desired, especially in the parametrization of the diabatic heating, and description of the process over the surface.

The equations were solved on a spherical latitude–longitude mesh, the grid intervals in the latitudinal and longitudinal direction being 5 degrees and 10 degrees respectively. The calculation domain was from 5°N–90°N. Centred differencing and the Arakawa advection scheme were used in calculating the spatial differences and the Jacobian terms. The main parameters of the model were taken as: $K_1 = 10\,\mathrm{m^2\,s^{-1}}$, $\tau_R = 3 \times 10^6\,\mathrm{s}$, $K_R = 0.05\,\mathrm{m^2\,s^{-1}}$, $K_s = 10^2\,\mathrm{cm^2\,s^{-1}}$ for the ocean and $0.005\,\mathrm{cm^2\,s^{-1}}$ for land.

6. Experiments in seasonal prediction

Two sets of eight seasonal predictions for the years 1981 to 1988 were carried out using the model. One set was for predictions from winter to summer, and the other from summer to winter. The predictions from winter to summer were initialized from January and predicted from February to August. The experiments from summer to winter were initialized from June and predicted from July to January. The historical data were based on the 1966–1980 data-set of 300 hPa, 500 hPa and 700 hPa geopotential heights and surface temperatures compiled by the Beijing Meteorological Centre. The basic states for the cases of winter to summer were obtained as follows. For a forecast initialized from the end of January for each year in the period 1981–1988, the best historical analogue to the January-mean anomaly was selected from all the January data in the historical record. The subsequent evolution of the general circulation as observed in the year selected was thus chosen as the basic state for the forecast month. The predicted anomaly was obtained by adding the deviation field predicted by the model to the corresponding anomaly in the basic state: a one-month prediction was taken as an average over 30 days. To check the forecast accuracy of the model, the 500 hPa geopotential and surface temperature monthly anomalies predicted by the model were compared with those observed, and skill scores, S_*, were compared with those for the statistical analogue forecasts, where $S_* = N/M$; M is the total number of gridpoints (540) and N is the number of gridpoints for which the sign of the anomaly was correctly predicted.

(*a*) *Prediction from winter to summer*

The skill scores for both the 500 hPa geopotential and the surface temperature monthly anomalies for February to August of the period 1981–1988 are shown in Table 1. The skill in most months is greater than 50%. However, 50% is an underestimate of the skill of a random forecast because the climatological error is present in both the forecast and observed anomalies. This is important to bear in mind in evaluating model forecast skill, especially in cases where the skill is itself expected to be small (Murphy and Dickinson 1990). The highest skill levels for the 500 hPa geopotential and surface temperature are 70% and 72% respectively. All the annual mean skill scores from February to August are also better than 50%; the highest skill levels for the 500 hPa geopotential and surface temperature are 59% and 58%, respectively. The average value of mean skill scores for 500 hPa geopotential and surface temperature are 56.8% and 55.4%, respectively.

The variation of the mean skill with latitude is shown in Fig. 3. It is found that the skill is better in low latitudes and in polar regions than in mid-high latitudes; for example the skill at 25°N reaches 61%.

TABLE 1. THE SKILL SCORES S_* (%) OF THE PREDICTION FROM WINTER TO SUMMER

Year		Feb.	Mar.	Apr.	May	June	July	Aug.	mean
1981	ϕ'	53	53	48	60	48	53	60	53.6
	T_s'	59	51	48	58	44	47	58	52.1
1982	ϕ'	60	48	53	54	55	57	58	55.0
	T_s'	55	53	50	51	48	54	57	52.6
1983	ϕ'	52	56	59	53	59	70	62	58.7
	T_s'	61	58	59	57	59	56	59	58.4
1984	ϕ'	55	50	51	54	65	69	65	58.4
	T_s'	54	60	49	61	55	62	55	56.6
1985	ϕ'	48	62	62	65	56	53	52	56.9
	T_s'	50	57	57	50	55	50	53	53.2
1986	ϕ'	51	58	65	64	59	60	56	59.0
	T_s'	58	58	55	53	50	61	55	55.7
1987	ϕ'	62	61	55	48	57	65	55	57.6
	T_s'	72	60	61	53	47	51	56	57.1
1988	ϕ'	46	58	55	51	50	69	57	55.1
	T_s'	50	56	57	51	53	58	57	54.6

ϕ' the 500 hPa geopotential anomaly, T_s' the surface temperature anomaly

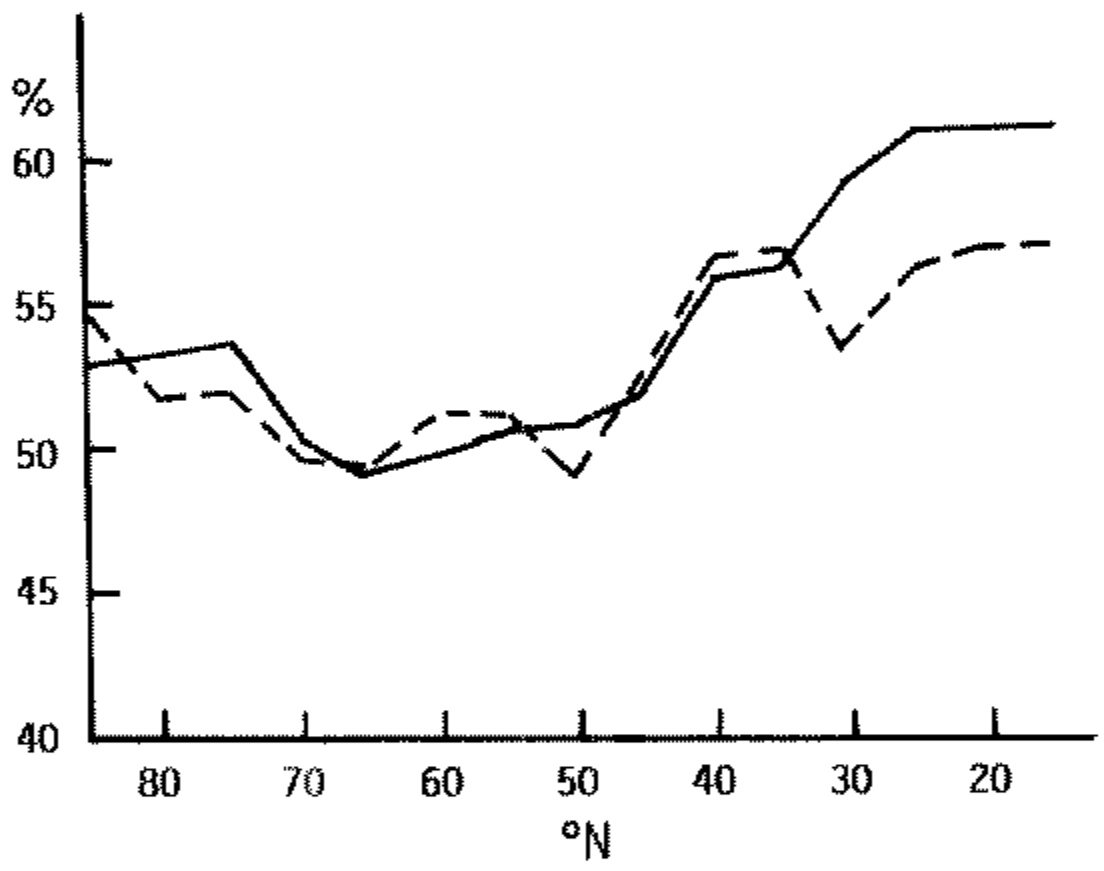

Figure 3. The variation of the mean skill score S_* (%) with latitude. Solid line: the anomaly of 500 hPa geopotential; dashed line: the anomaly of surface temperature.

Figure 4(a,b) shows the predicted and observed maps for the anomaly field of 500 hPa geopotential height for June 1983. By comparison between (*a*) and (*b*) we see that the positive anomaly centres were well predicted, but the negative centres over the polar regions and mid latitudes of the Pacific were not, instead a false negative centre appeared over the western coast of North America. There were also some quantitative differences between the predicted and observed; in particular, the values of the predicted anomalies were too small.

Figure 5(a,b) shows the predicted and observed maps for the anomaly field of the 500 hPa geopotential height for July 1983. In both (*a*) and (*b*) we see a fair agreement in the general pattern. The model predicted the negative anomalous region over the eastern coast of North America quite successfully.

Figure 6(a,b) shows the predicted and observed maps for the anomaly field for the 500 hPa geopotential height for August 1983. The negative anomalies over polar regions were in agreement with the observations, however, the positive anomaly over the Aleutians was not predicted.

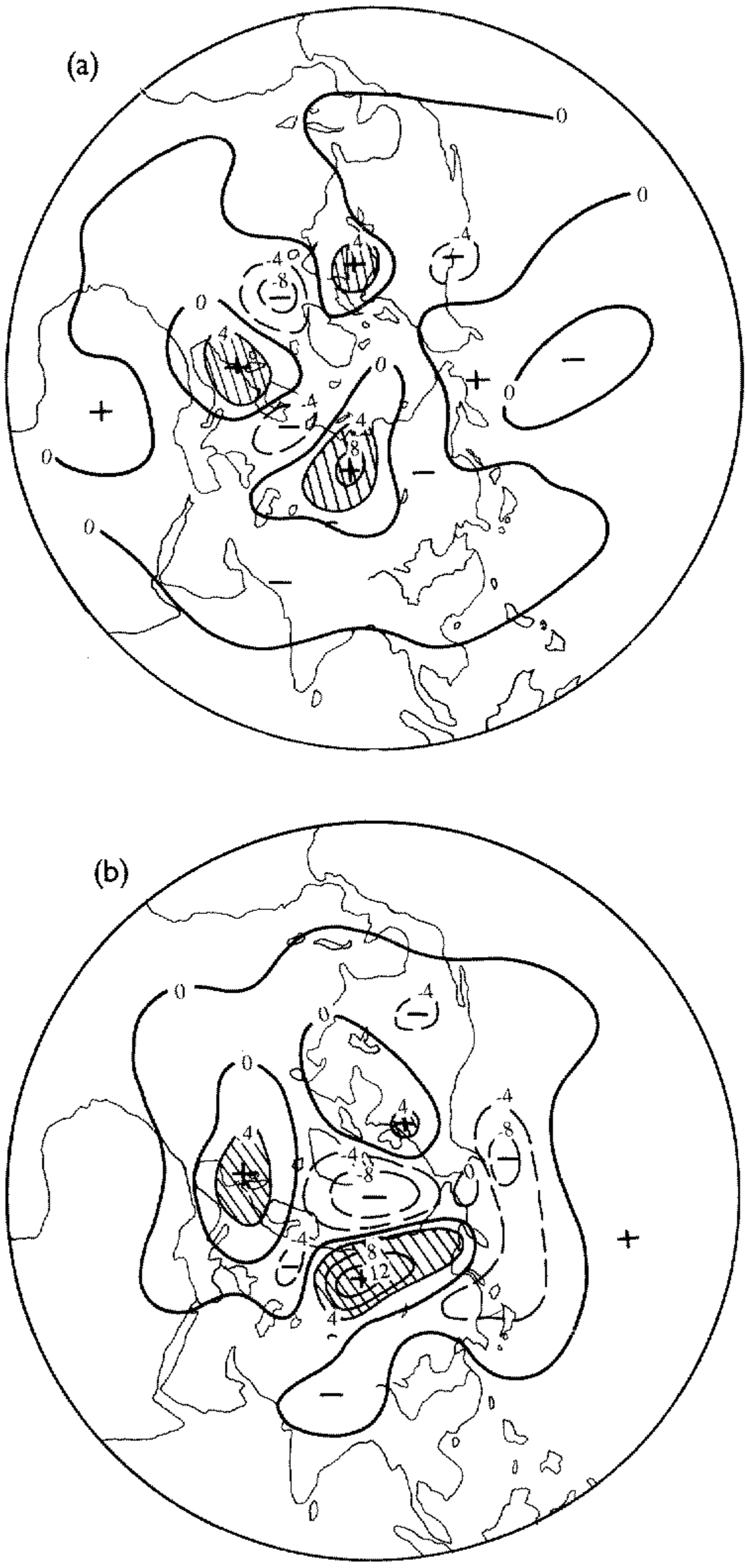

Figure 4. (a) The predicted anomaly field of 500 hPa height for June 1983. (b) The observed anomaly field of 500 hPa height for June 1983.

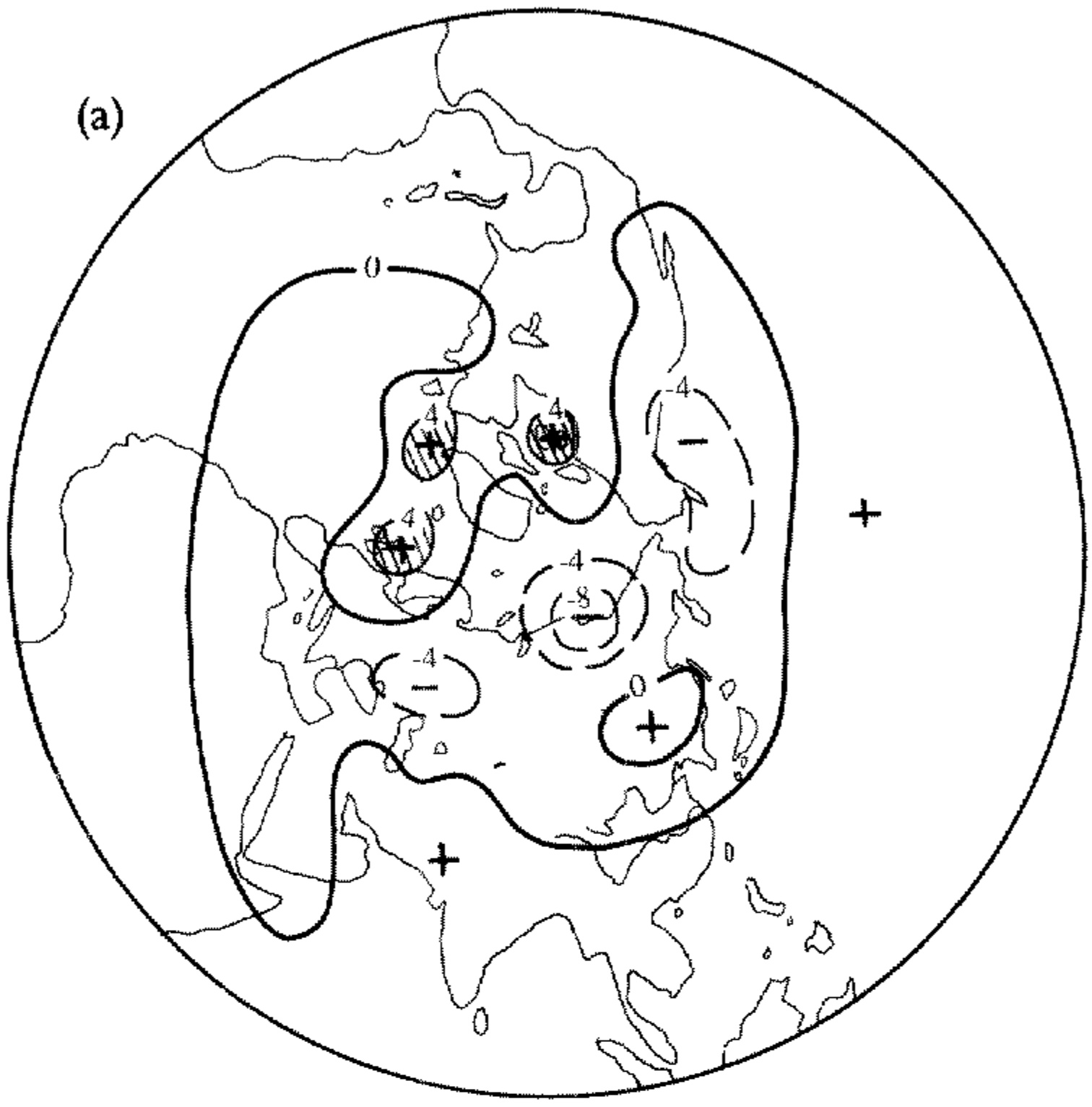

Figure 5. As in Fig. 4(a,b), but for July 1983.

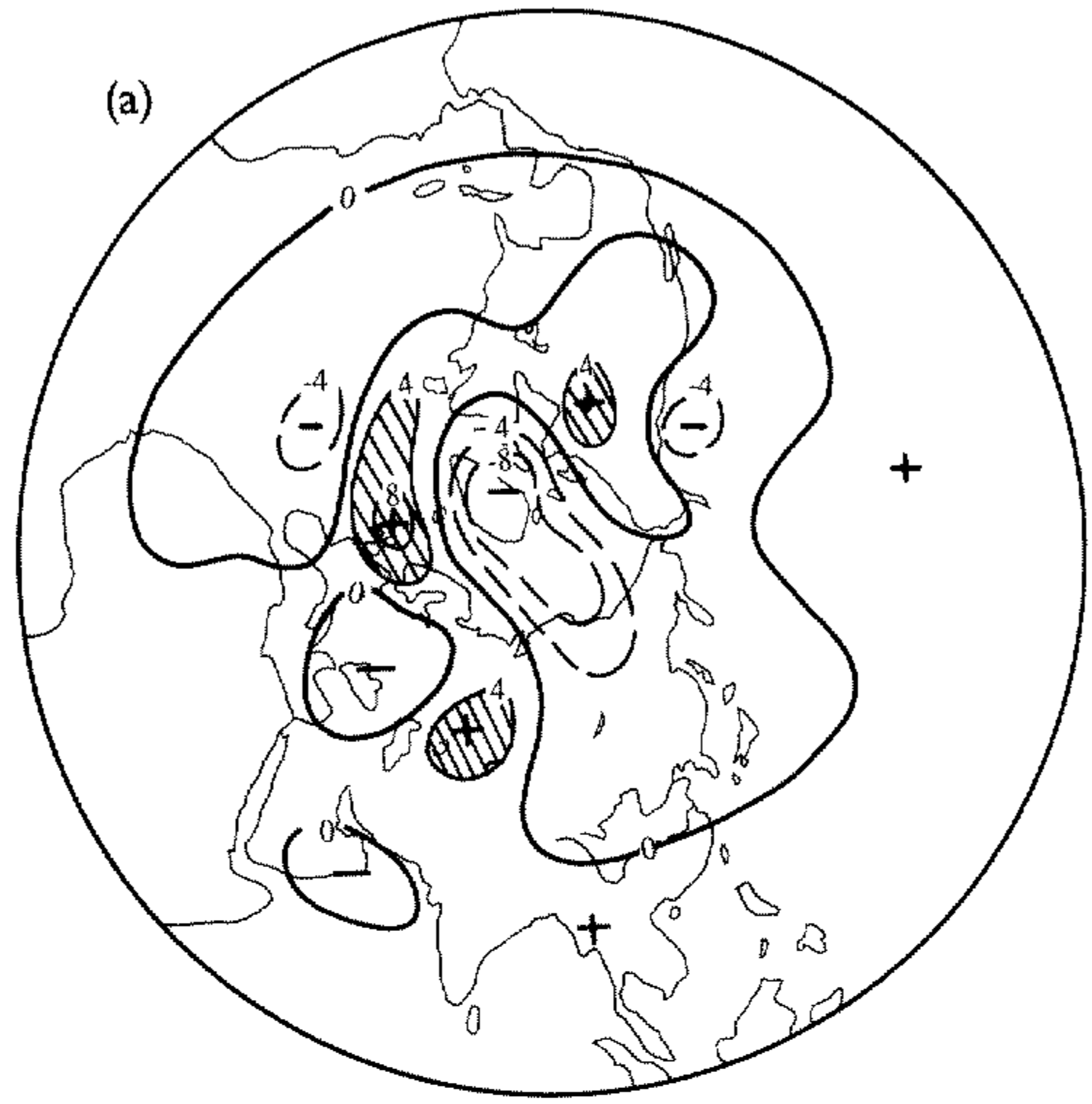

Figure 6. As in Fig. 4(a,b), but for August 1983.

The results of the model predictions were also compared with simple analogue forecasts. The analogue forecasts used for this purpose consisted of the anomalous basic-state fields selected from the historical data-set according to their similarity in winter (also used to represent the evolution of the historical analogue field in the forecast). The mean skill of the predictions by the model and by the simple analogue methods are shown in Fig. 7 from which it is seen that whereas the predictions by the model were, in general, better than the simple analogue forecasts, especially in the summer months, the

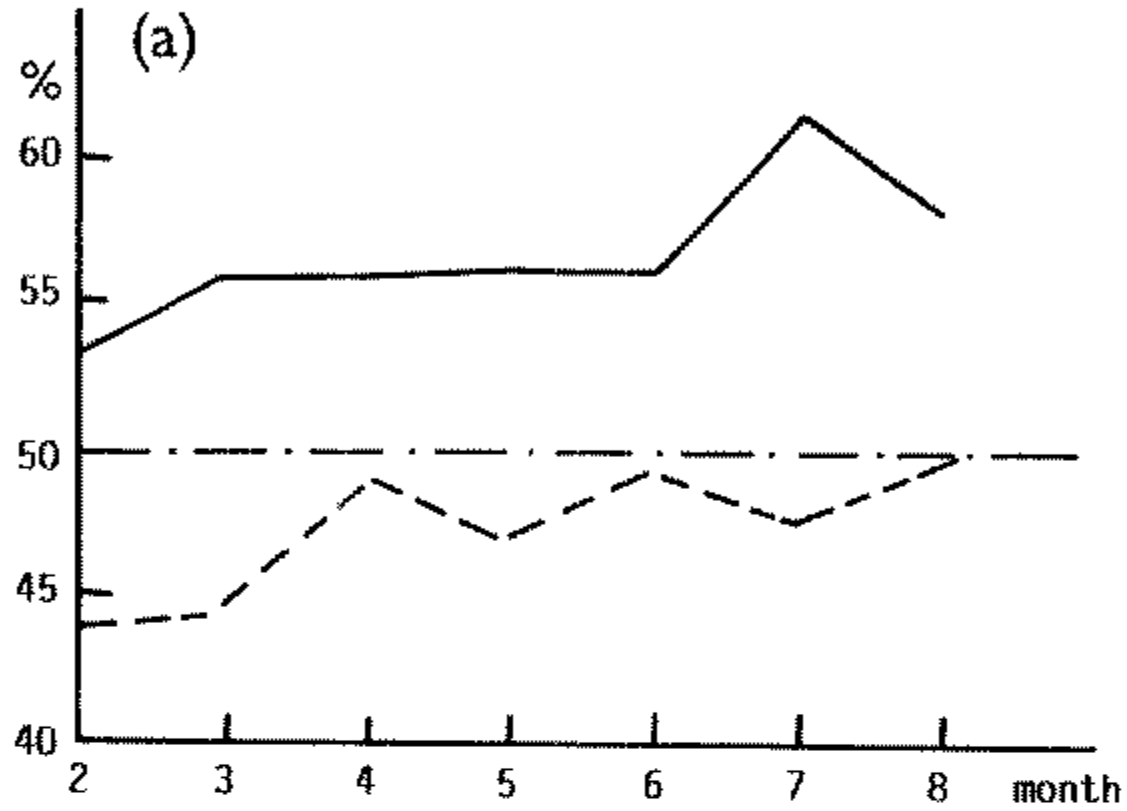

Figure 7. The mean skill score S_* (%) of the model (solid line), and analogue (dashed line) predictions for (a) 500 hPa geopotential and (b) surface temperature.

skill of the simple analogue was a little worse than that of a random forecast; even although this skill was the average for eight cases—not for a single experiment. In a few experiments however the skill of the simple analogue prediction was better than the average. On the other hand, the series used in searching for the analogues was not large enough; the skill of the simple analogue prediction might have been higher than that presented in Fig. 7 if only the data-set had been updated. Therefore, Fig. 7 indicates only that the skill of the model predictions showed some improvement over those based on simple analogues. The analogue–dynamical approach might have produced higher skills if better analogues had been selected.

(*b*) *Predictions from summer to winter*

The skill scores for both 500 hPa geopotential and surface temperature monthly anomalies from the months July to January during the period 1981–1988 are shown in Table 2. It is seen that 90% of the results have skill scores exceeding 50% (with 40% exceeding a skill score of 60%). The highest skill score for the 500 hPa geopotential and the surface temperature are 73.4% and 70%, respectively. In addition, the mean skills during the autumn months are better than those of the winter months.

TABLE 2. THE SKILL SCORES S_* (%) OF THE PREDICTION FROM SUMMER TO WINTER

Year		July	Aug.	Sept.	Oct.	Nov.	Dec.	Jan.	mean
1981	ϕ'	53	56	73	58	57	72	53	60.3
	T_s'	60	59	61	57	52	61	56	58.0
1982	ϕ'	49	55	69	52	57	61	64	58.1
	T_s'	67	62	63	64	56	50	62	60.6
1983	ϕ'	65	68	71	62	67	62	61	65.1
	T_s'	65	67	65	62	64	55	53	61.6
1984	ϕ'	66	53	58	53	48	65	72	59.3
	T_s'	54	60	55	55	57	67	64	58.9
1985	ϕ'	66	59	55	71	57	59	70	62.4
	T_s'	62	65	54	71	58	60	55	60.7
1986	ϕ'	59	65	51	54	50	52	46	53.9
	T_s'	63	61	55	54	53	49	49	54.9
1987	ϕ'	67	64	64	53	63	68	67	63.7
	T_s'	61	53	63	46	53	56	48	54.3
1988	ϕ'	67	47	58	52	65	57	55	57.3
	T_s'	68	59	60	66	69	58	56	62.4

ϕ' the 500 hPa geopotential anomaly, T_s' the surface temperature anomaly

Figure 8(a,b) shows the predicted and observed maps for the anomaly field of 500 hPa geopotential height for October 1985. Comparing Fig. 8(a) and Fig. 8(b) we see that the regions with positive and negative predicted anomalies were similar to the observed, except in eastern Asia, but the intensity of the predictions was rather smaller than observed.

Figure 9(a,b) shows the predicted and observed maps for the anomaly field of the 500 hPa geopotential height for January 1986. Comparison between Fig. 9(a) and Fig 9(b) shows that the predicted patterns were close to those observed, but with a smaller magnitude.

7. CONCLUSIONS AND FUTURE WORK

It is generally accepted that the theoretical limitation of daily predictions is 2–3 weeks. For the monthly mean circulation, we consider the theoretical limitation to be 6–11 months. Because of climatic noise, however, the theoretical prediction accuracy can only be achieved to a limited extent. The use of a coupled numerical forecasting atmosphere–ocean model in this respect has some disadvantages, such as the differences between the model's representations of the underlying ocean (or land) surface and the observed data. In this paper we have advanced a prediction method which attempts to establish a simple model to describe the anomaly evolution of the monthly mean circulation. The historical data of the circulation's evolution is used to remedy the disadvantage caused by the lack of three-dimensional data for the active surface layer. Also the accumulated experience from the use of statistical prediction is applied. The

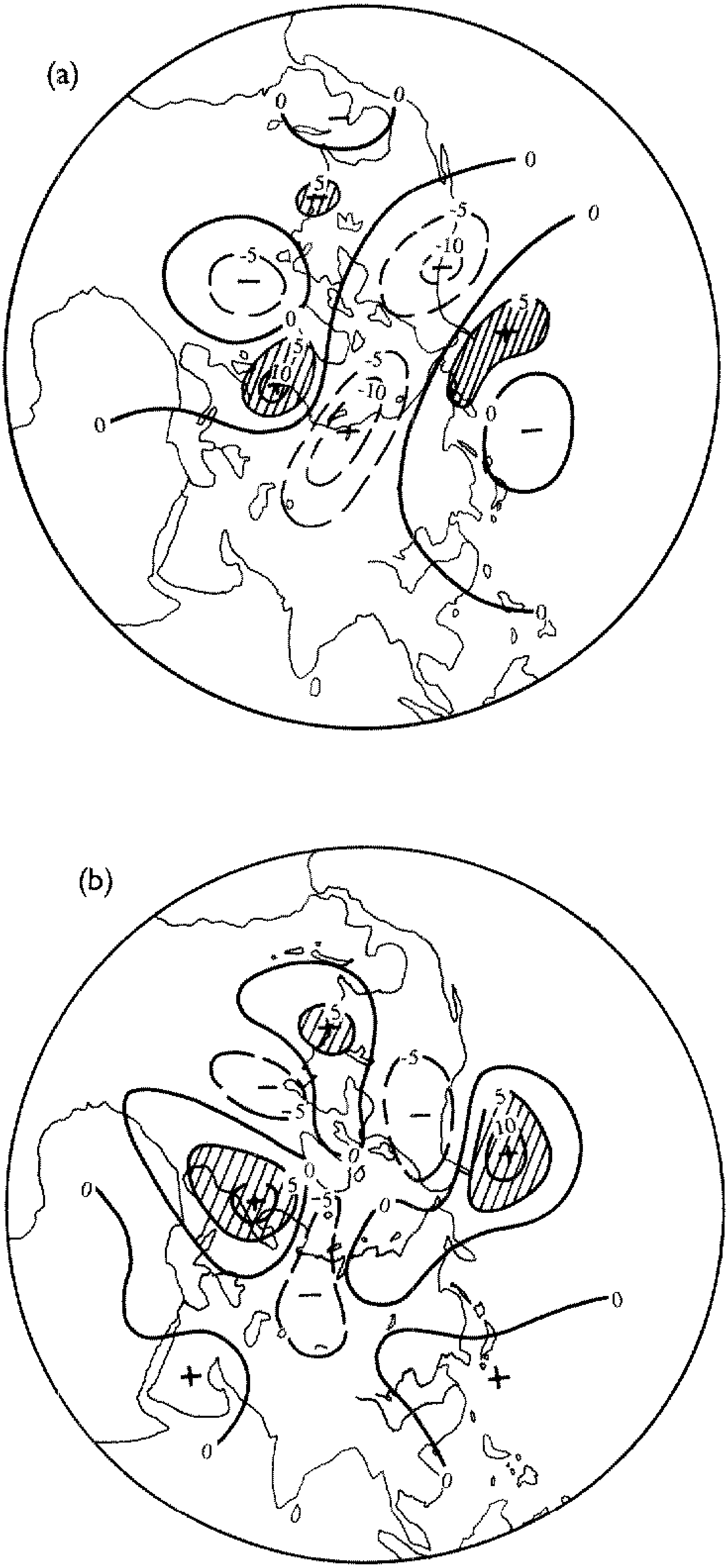

Figure 8. As in Fig. 4(a,b), but for October 1985.

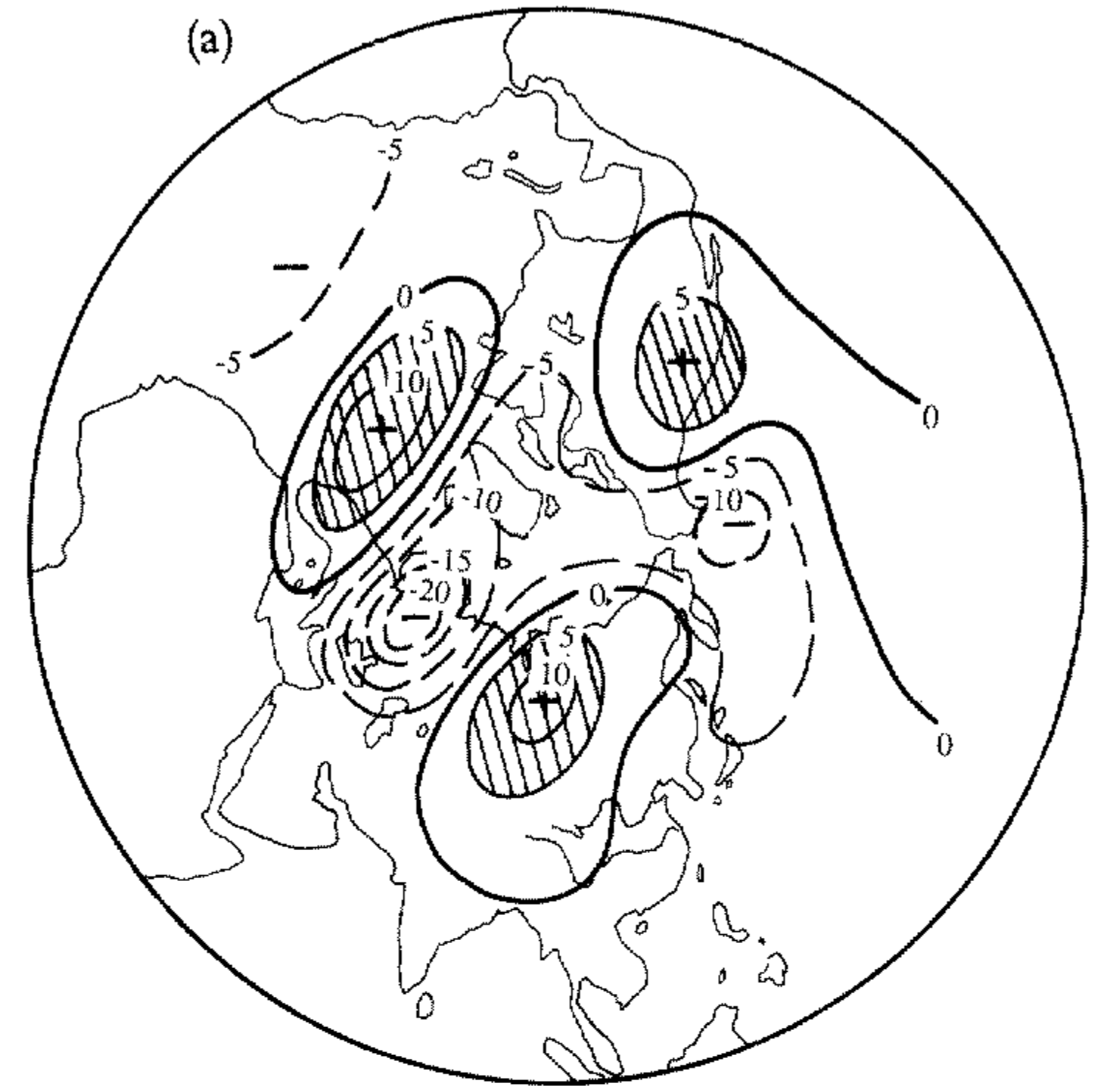

Figure 9. As in Fig. 4(a,b), but for January 1986.

preliminary results of the experiments show that the analogue–dynamical model has some capability for seasonal prediction.

However, many discrepancies are apparent, most notably that the values of the predicted anomalies are too small. These errors may be connected with the unrealistic parametrizations and with the method of selection of the historical analogue fields.

Further extensions of this work that could possibly bring improvements are the following:

(a) The introduction of more realistic parametrizations and a better construction for the analogue–dynamical model. Although the parameters can be determined from observed data, whether or not the parametrization scheme itself conforms with reality still needs to be examined more carefully. The method suggested here may not be the best.

(b) Collection over a long period of historical data, and improvements in the analogue selection procedures. Experiments show that the prediction skill is greatly improved over that based on statistical analogues only, but the analogue field (i.e. the basic state) has a very important influence on the accuracy of the predictions. However, the analogue selection technique used here is very simple and only 15 years of data were available as historical data; this does not seem to be a long enough period for the selection of analogues to be satisfactory.

In conclusion, it can be stated that we are aiming to develop a new version with more realistic parametrizations of diabatic heating and with an improved treatment of the oceanic active layer.

Acknowledgements

We are indebted to the referees. The paper was substantially improved by the comments of two anonymous referees. This research is supported by the National Key Fundamental Program of China in connection with the project for climate dynamics and predictions.

References

Barnett, T. P. and Preisendorfer, R. W. 1978 Multifield analogy prediction of short-term fluctuations using a climate state vector. *J. Atmos. Sci.*, **35,** 1771–1787

Blackmon, M. L., Madden, R. A., Wallace, J. M. and Gutzler, D. S. 1979 Geographical variation in the vertical structure of geopotential height fluctuations. *J. Atmos. Sci.*, **36,** 2450–2466

Chou, J. F. 1986a Why need we combine dynamics with statistics in long-range weather forecasting? *Plateau Meteorol.*, **5,** 367–372, (in Chinese)

Chou, J. F. 1986b Long-range numerical weather prediction, *Meteorol. Press* (in Chinese)

Chou, J. P., Jih, C. C., Ho, C. H., Liu, K. W., Lu, Y. H., Chou, C. F., Pei, C. T., Pan, H. S., Hsuan, T. W., Hung, M. H., Chung, Y. C. and Wei, H. 1977 On the physical basis of a model of long-range numerical weather forecasting. *Scientia Sinica*, **20,** 377–390

Chou, J. P., Guo, Y. F. and Xin, R. N. 1982 A theory and method of long-range numerical weather forecasts, *J. Meteorol. Soc. Jpn.*, **60,** 282–291

Davis, N. E. 1978a The summer of 1978. *Weather*, **33,** 197

1978b Prospects for winter 1978/79. *Weather*, **33,** 480

Folland, C. K. 1975 A relationship between cool summers in central England and the temperature of the following winter for summers occurring in an even year, *Weather*, **30,** 348–358

Gruza, G. V. and Rankova, E. Y. 1980 Long-range weather forecasting using a group of analogues and evaluation of meteorological predictability. Proc. WMO Symp. on probabilistic and statistical methods in weather forecasting, Nice, September 1980.

Huang, J. P. and Chou, J. F. 1988 On the annual variation of the barotropic and baroclinic energy for northern hemisphere monthly mean circulation. *Plateau Meteorol.*, **7,** 264–268 (in Chinese)

1990 The studies on the analogous rhythm phenomenon in a coupled ocean–atmosphere system. *Scientia Sinica*, **33,** 851–860

Jolliffe, I. T. 1979 Not very good. *New Sci.*, **84,** 192–194

Kuo, H. L. 1969 On a simplified radiative-conductive heat transfer equation, Proc. WMO/IUGG Symp. on numerical weather prediction 1968, Japan Meteorological Agency, Tokyo

Lee, D. and Ratcliffe, R. A. S. 1976 Objective method of long-range forecasting using surface pressure anomalies. *Weather*, **31,** 56–65

Lin Benda, Xu, X. D. and Wang, S. W. 1988 Preliminary experiments from a nonsteady atmosphere–earth surface coupled anomaly model. *Acta Oceanol. Sinica*, **7,** 369–380

Lorenz, E. N. 1969 Atmospheric predictability as revealed by naturally occurring analogues, *J. Atmos. Sci.*, **26,** 636–646

Miyakoda K. and Chao, J. P. 1982 Essay on dynamical long-range forecasts of atmospheric circulation, *J. Meteorol Soc. Jpn.*, **60,** 292–308

Murphy, J. M. and Dickinson, A. 1990 Extended-range prediction experiments using an 11-level GCM. *Meteorol. and Atmos. Phys.*, **40,** 61–83

Murray, R. 1968 Some predictive relationships concerning seasonal rainfall over England and Wales and seasonal temperatures in central England. *Meteorol. Mag.* **97,** 303–310

1972 An objective method of foreshadowing winter rainfall and temperature for England and Wales. *Meteorol. Mag.* **101,** 97–110

1973 Forecasting seasonal rainfall and temperature for England and Wales in spring and autumn from anomalous atmospheric circulation over the northern hemisphere. *Meteorol. Mag.*, **102,** 15–26

1974 Indicators of monthly mean temperatures and rainfall for England and Wales based on antecedent monthly pressure anomalies over the northern hemisphere. *Meteorol. Mag.*, **103,** 70–73

1977 The accuracy of seasonal forecast based on pressure anomaly rules. *Weather*, **32,** 325–326

Murray, R. and Benwell, P. R. 1970 PSCM indices in synoptic climatology and long-range forecast. *Meteorol. Mag.*, **99,** 232–245

Nap, J. L., Van den Dool, H. M. and Oelemans, J. 1981 A verification of monthly weather forecasts in the seventies, *Mon. Weather Rev.*, **109,** 306–312

Navarra A. and Miyakoda, K. 1988 Anomaly general circulation models. *J. Atmos. Sci.*, **45,** 1509–1530

Nicholls, N. 1984 Long-range weather forecasting: recent research. In Long-range forecasting research publications series No. 3

Ratcliffe, R. A. S. 1968 Forecasting monthly rainfall for England and Wales. *Meteorol. Mag.* **97,** 258–270

1974 The use of 500 mb anomalies in long-range forecasting. *Q. J. R. Meteorol. Soc.*, **100,** 234–244

Ratcliffe, R. A. S. and Collison, P. 1969 Forecasting rainfall for the summer season in England and Wales. *Meteorol. Mag.* **98,** 33–39

Schuurmans, C. J. E. 1973 A 4-year experiment in long-range weather forecasting using circulation analogues. *Meteorol. Rdsch.*, **26,** 2–4

Smagorinsky, J. 1969 Problems and promises of deterministic extended range forecasting. *Bull. Am. Meteorol. Soc.*, **150,** 286–311

Wang, S. W. 1984 The rhythm in the atmosphere and ocean in application to long-range weather forecasting. *Adv. Atmos. Sci.*, **1,** 7–18

Wang, S. W. and Zhao, Z. C. 1987 Basic theory of long-range forecasting. *Sci. Tech. Press*, Shanghai (in Chinese)